Kinetic and Structural Characterization of Phosphofructokinase from Lactobacillus bulgaricus †

ARTICLE *in* BIOCHEMISTRY · DECEMBER 2005

Impact Factor: 3.02 · DOI: 10.1021/bi051283g · Source: PubMed

Kinetic and Structural Characterization of Phosphofructokinase from *Lactobacillus bulgaricus*†

N. Monique Paricharttanakul, Sheng Ye, Ann L. Menefee,‡ Farah Javid-Majd, James C. Sacchettini, and Gregory D. Reinhart*

Department of Biochemistry and Biophysics, Texas A&M University, and the Texas Agricultural Experiment Station, College Station, Texas 77843-2128

Received July 5, 2005; Revised Manuscript Received September 12, 2005

ABSTRACT: Phosphofructokinase from *Lactobacillus delbrueckii* subspecies *bulgaricus* (LbPFK) has been reported to be a nonallosteric analogue of phosphofructokinase from *Escherichia coli* at pH 8.2 [Le Bras et al. (1991) *Eur. J. Biochem. 198*, 683−687]. A reexamination of the kinetics of this enzyme shows LbPFK to have limited binding affinity toward the allosteric ligands, MgADP and PEP, with dissociation constants of approximately 20 mM for both. Their allosteric effects are observed only at high concentrations of these ligands, with both exhibiting inhibitory effects on substrate binding. No pH dependence was observed for the binding and the influence of MgADP and PEP on the enzyme. To attempt to explain these results, the crystal structure of LbPFK was solved using molecular replacement to 1.86 Å resolution. A comparative study of the LbPFK structure with that of phosphofructokinases from *E. coli* (EcPFK) and *Bacillus stearothermophilus* (BsPFK) reveals a structure with conserved fold and substrate binding site. The effector binding site, however, shows many differences that could explain the observed decreases in binding affinity for MgADP and PEP in LbPFK as compared to the other two enzymes.

Phosphofructokinase (PFK[1]) catalyzes the first irreversible step in the glycolytic pathway and is allosterically regulated by small metabolites. Bacterial PFKs respond to changing levels of MgADP and phospho(enol)pyruvate (PEP) (*1*−*5*). These molecules compete for binding to the same allosteric site in the enzyme with different effects. MgADP activates PFK by increasing the binding affinity for Fru-6-P in the active site while PEP inhibits the binding of Fru-6-P. The means by which the enzyme can differentiate which molecule is bound and respond appropriately remains a compelling question.

Phosphofructokinases from *Escherichia coli* (EcPFK) and *Bacillus stearothermophilus* (BsPFK) are two of the most extensively characterized bacterial PFKs. Investigations into their allosteric properties and structures have been performed to probe the basis for allosteric regulation (*3*, *6*). The crystal structures of these enzymes have been solved, and they show a high degree of similarity to one another (*7*, *8*).

Phosphofructokinase from *Lactobacillus delbrueckii* subspecies *bulgaricus* (LbPFK) contains 47% amino acid sequence identity and 66% similarity to EcPFK, and 56% identity and 74% similarity to BsPFK. Interestingly, LbPFK has been reported to be unresponsive to allosteric ligands at pH 8.2 (*9*). According to that study, the maximal activity of the enzyme is influenced by pH. The activity of LbPFK was inhibited by the presence of 8 mM and 20 mM PEP only at low pH values. ADP or GDP binding was not observed. From these data, it was concluded that LbPFK is a nonallosteric enzyme at high pH.

The study presented here describes a more thorough investigation into the kinetic properties of PFK from *L. bulgaricus* using a linked-function approach (*10*, *11*). In addition, we present the crystal structure of LbPFK, determined to 1.86 Å resolution, to allow the study of the three-dimensional structural features of this enzyme. A comparative analysis of the structure and function relationship between LbPFK and the extensively studied PFKs from *E. coli* and *B. stearothermophilus* may facilitate our understanding of the allosteric response mechanisms of these enzymes.

MATERIALS AND METHODS

Materials. PFK from *L. bulgaricus* B107, cloned into pKK223-3, was kindly provided by Danone Vitapole SA, France (*12*). All chemical reagents were analytical grade, purchased from Fisher Scientific or Sigma-Aldrich. The sodium salts of Fru-6-P, PEP, NADH, and phosphocreatine and the potassium salt of ADP were purchased from Sigma-Aldrich. Creatine kinase, aldolase, glycerol-3-phosphate dehydrogenase, the sodium salt of ATP, and DTT were purchased from Roche Applied Science. Mimetic Blue 1 agarose resin for protein purification was purchased from Prometic BioSciences. DE-52 resin was obtained from

† This work was supported by National Institutes of Health Grant GM33216 and Robert A. Welch Foundation Grant A1543.

* Author to whom correspondence should be addressed. E-mail: gdr@tamu.edu.

‡ Current address: Department of Biochemistry, University of Wisconsin−Madison.

[1] Abbreviations: DTT, dithiothreitol; EPPS, *N*-(2-hydroxy-ethyl)-piperazine-*N*′-(3-propanesulfonic acid); MES, 2-(*N*-morpholino)ethanesulfonic acid; MOPS, 3-(*N*-morpholino)propanesulfonic acid; Fru-6-P, fructose 6-phosphate; Fru-1,6-BP, fructose 1,6-bisphosphate; PEP, phospho(enol)pyruvate; PFK, phosphofructokinase; EcPFK, phosphofructokinase I from *Escherichia coli*; BsPFK, phosphofructokinase I from *Bacillus stearothermophilus*; LbPFK, phosphofructokinase I from *Lactobacillus bulgaricus*.

10.1021/bi051283g CCC: $30.25
Published on Web 10/28/2005

Whatman. Crystallization materials were purchased from Hampton Research. Bicinchoninic acid (BCA) protein assay reagents were purchased from Pierce.

Protein Purification. pKK223-3/PFK was transformed into DF1020 cells for overexpression of the PFK gene in a PFK minus strain (*13*). Cells were grown up in LB broth in the presence of 0.1 mg/mL ampicillin at 37 °C, harvested after 24 h, and stored at −20 °C. The harvested cells were resuspended in buffer B (10 mM Tris-HCl pH 7.2, 0.1 mM EDTA), sonicated, and centrifuged. The clarified lysate was treated with DNAse I and centrifuged, and the resulting lysate was loaded onto preequilibrated Mimetic Blue 1 resin. The column was washed with at least two column volumes with buffer before PFK was eluted with a NaCl gradient from 0 to 2 M in the same buffer. PFK eluted at approximately 1 M NaCl. Fractions containing PFK were pooled, dialyzed against buffer A (50 mM Tris-HCl pH 7.5, 5 mM $MgCl_2$, 0.1 mM EDTA, 2 mM DTT), and concentrated. The purity of LbPFK at this point was sufficient for kinetic characterization; however, an additional purification step was required for crystallization trials. The concentrated protein was loaded onto a preequilibrated DE-52 anion exchange column. PFK was then eluted from the anion-exchange column at approximately 0.26 M NaCl using a 0 to 1 M NaCl gradient in buffer A. Fractions containing PFK were pooled, dialyzed against buffer A, concentrated, and stored at 4 °C. Protein concentration was determined by using the BCA protein assay. Protein purity was assessed by SDS−PAGE.

Kinetic Assays. Standard PFK activity assays were performed at pH 8.0 and 25 °C unless otherwise noted. The production of fructose-1,6-bisphosphate was monitored by the oxidation of NADH using a coupled-enzyme system. The reaction was initiated by the addition of 6 μL of appropriately diluted PFK to a total assay volume of 600 μL of V_{max} buffer (50 mM EPPS pH 8.0, 10 mM $MgCl_2$, 10 mM NH_4Cl, 0.1 mM EDTA), 2 mM DTT, 250 μg of aldolase, 50 μg of glycerol-3-phosphate dehydrogenase, and 25 mg of triose phosphate isomerase. MES and MOPS were used in the V_{max} buffer for pH 6 and pH 7, respectively. 15 mM MgATP and 5 mM Fru-6-P were used to achieve maximal activity of the enzyme. Fru-6-P, MgATP, MgADP, and PEP concentrations were varied as indicated. MgATP was added as a solution of equal concentrations of $MgCl_2$ and ATP. MgADP was added as a solution of equal molar MgADP/MgATP to prevent product inhibition by MgADP from complicating the interpretation of results. In the absence of MgADP, 40 μg/mL creatine kinase and 4 mM phosphocreatine were added to the assay mixture as an ATP regeneration system to avoid the accumulation of ADP. The rate of the reaction is measured by the decrease of absorbance at 340 nm as a function of time. One unit of enzyme activity is defined as the amount of enzyme needed to produce 1 μmol of fructose-1,6-bisphosphate per minute.

Data Analysis. Data were fit to appropriate equations using the nonlinear least-squares fitting analysis of Kaleidagraph software (Synergy). Initial rates as a function of either Fru-6-P or MgATP concentrations were fit to the Michaelis Menten equation (*14*),

$$\frac{v}{E_T} = \frac{k_{cat}[A]}{K_a + [A]} \quad (1)$$

where v = initial rate, E_T = total enzyme active site concentration, k_{cat} = turnover number, A = substrate Fru-6-P or MgATP, and K_a = the Michaelis constant for substrate A. In the presence of substrate inhibition, data were fit to the following equation (*14*):

$$\frac{v}{E_T} = \frac{k_{cat}[A]}{K_a + [A] + [A]^2/K_i} \quad (2)$$

where K_i is the inhibition constant.

To quantify the allosteric responses of PFK to MgADP, parameters obtained from the fit to eq 1 were further fit to the following equation (*10*):

$$K_a = K_a^\circ\left[\frac{K_{ix}^\circ + [X]}{K_{ix}^\circ + Q_{ax}[X]}\right] \quad (3)$$

where X is MgADP, K_a° is the Michaelis constant for Fru-6-P in the absence of MgADP, and K_{ix}° is the dissociation constant for MgADP in the absence of Fru-6-P. The coupling constant Q_{ax} describes the nature and magnitude of the allosteric response (*10*, *11*). Q_{ax} will be greater than 1 when MgADP acts as an activator of Fru-6-P binding, and Q_{ax} is less than 1 when MgADP causes inhibition of Fru-6-P binding. When Q_{ax} is equal to 1, there is no allosteric response. When MgADP exhibits inhibition and its binding is very weak, as occurs in LbPFK, MgADP saturation at the allosteric site cannot be achieved, and the data were instead fit to the following competitive inhibition equation (*14*), which corresponds to eq 3 at relatively low concentrations of X:

$$K_a = K_a^\circ\left(1 + \frac{[X]}{K_{ix}^\circ}\right) \quad (4)$$

Finally, by convention, when eqs 3 and 4 are applied to the allosteric action of PEP, the subscripts are changed to "*y*", and PEP is designated as "Y", to be consistent with the notation we have used previously (*5*).

Crystallization and Data Collection. PFK from *L. bulgaricus* was crystallized at 18 °C using the hanging drop vapor diffusion method with 4 μL hanging droplet consisting of a 1:1 mixture of the stock protein solution and the reservoir solution (0.1 M Tris HCl pH 7.5, 1 mM DTT, at 0.1 M increments of 0.8 M to 1.4 M ammonium sulfate). Within 48 h, PFK crystals were observed in all wells and were hexagonal in shape. Crystals, grown in 1.2 M ammonium sulfate, were flash frozen at 100 K using 20% ethylene glycol as cryoprotectant, and X-ray diffraction data was collected at the Advanced Photon Source (APS) beamline in Chicago. Diffraction data were processed and analyzed using HKL2000 programs (*15*).

Structure Determination, Modeling Building, and Refinement. Molecular replacement program AMoRe (*16*) was used to solve the structure of PFK of *L. bulgaricus* using PFK structure of *Bacillus stearothermophilus* (*17*) as a model. A clear solution with correlation coefficient of 42.9% was obtained from AMoRe. Iterative cycles of model building with XtalView (*18*) using the ARPwARP improved phases figure of merit weighted $2|F_o| - |F_c|$ maps (*19*) and refinement with REFMAC (*16*) were performed for improving the quality of the model. Water molecules were added

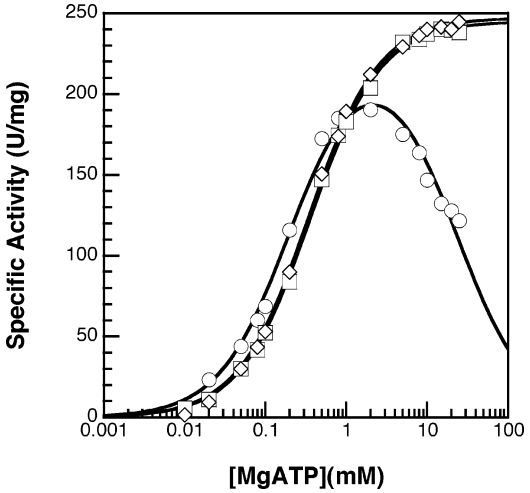

FIGURE 1: Kinetic characterization of LbPFK as a function of MgATP at pH 8 in the presence of 0.02 mM (○), 5 mM (□) and 10 mM (◇) Fru-6-P concentrations. Data for 0.02 mM Fru-6-P were fit to eq 2, while the others were fit to eq 1.

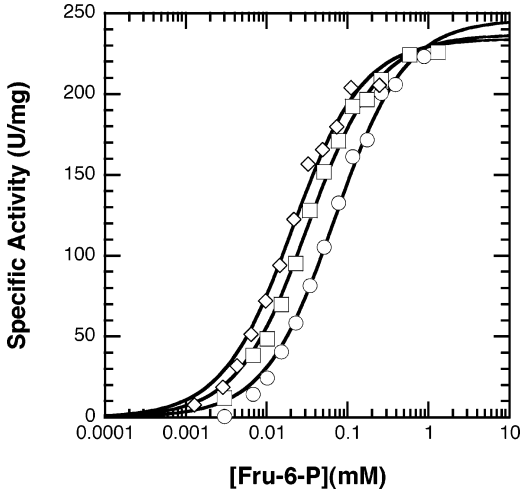

FIGURE 2: Fru-6-P dependence of LdPFK activity at pH 6 (○), pH 7 (□), and pH 8 (◇) with MgATP concentration equal to 15 mM. Lines represent best fits to eq 1.

in the difference electron density maps at positions corresponding to peaks (>3.0σ) and with appropriate hydrogen bonding geometry.

RESULTS

Kinetic Characterization. PFK from *L. bulgaricus* was purified to homogeneity as assessed by SDS−PAGE using affinity and anion-exchange chromatography.

When MgATP is the variable substrate, substrate inhibition is evident at low concentrations of Fru-6-P but not at high Fru-6-P concentrations as shown in Figure 1. This inhibition is similar to that observed previously for PFK from *E. coli* and *B. stearothermophilus* (*20*, *21*). At high concentrations of Fru-6-P, the kinetic response to MgATP is hyperbolic, and the data fit well to eq 1. When Fru-6-P is saturating, the K_a for MgATP is 0.35 mM and the specific activity is 240 units/mg at pH 8. This specific activity is roughly 2-fold higher than that obtained by Le Bras et al. (*9*). Most of the data reported by Le Bras et al. were obtained with the MgATP concentration fixed at 2 mM, which would only produce 85% of the maximal activity based upon our data. In addition, we note that our assays included the monovalent cation NH_4^+, which enhances specific activity by more than 60% (data not shown). These two effects are sufficient to account for the greater activity that we measured.

The dependence of activity on Fru-6-P concentration is presented in Figure 2 with MgATP concentration fixed at 15 mM. The data are reasonably well fit by the Michaelis Menten equation, although a small deviation at low Fru-6-P concentrations is evident reflecting the MgATP substrate inhibition shown in Figure 1. When the pH is lowered from 8 to 6, the K_a for Fru-6-P increases from 21 μM to 70 μM, although k_{cat} remains essentially constant. Except for the pH dependence of the K_a for Fru-6-P, none of the initial velocity characteristics are remarkably different from those of either EcPFK or BsPFK, although EcPFK does display more pronounced positive cooperativity in its Fru-6-P saturation profiles (*20*).

Allosteric Properties. In Figure 3 we contrast the influence of PEP and MgADP on the K_a for Fru-6-P of LbPFK with EcPFK and BsPFK at pH 8 and 25 °C. It is evident that

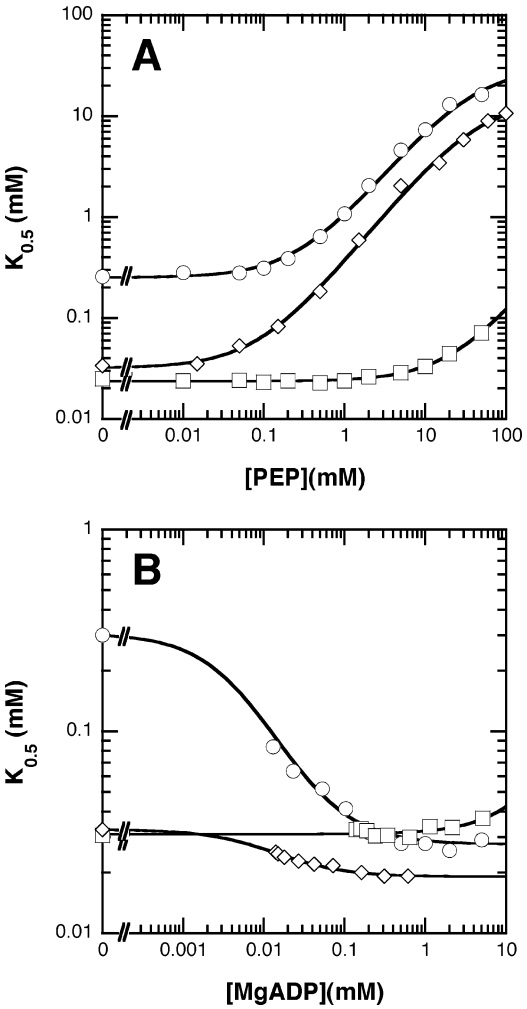

FIGURE 3: The effect of allosteric effectors on EcPFK (○), LdPFK (□), and BsPFK (◇) on Fru-6-P binding at pH 8 and 25 °C. (A) PEP; (B) MgADP. Lines represent best fits to eq 3 for EcPFK and BsPFK, and to eq 4 for LbPFK. $K_{0.5}$ represents the concentration of Fru-6-P that produces one-half maximal velocity and is equal to K_a for BsPFK and LdPFK.

PEP binds very weakly to LbPFK compared to the other two enzymes. Due to this low affinity, the extent of inhibition cannot be determined because of the inability to saturate the

Table 1: Summary of Kinetic Parameters for EcPFK, BsPFK, and LbPFK at pH 8 and 25 °C[a]

	$K_a°$ (mM)	K_{ix} (mM)	Q_{ax}	$K_{iy}°$ (mM)	Q_{ay}
EcPFK	0.30 ± 0.01	0.048 ± 0.002	11.1 ± 0.2	0.30 ± 0.01	0.0080 ± 0.0003
BsPFK[b]	0.031 ± 0.002	0.019 ± 0.002	1.7 ± 0.1	0.093 ± 0.006	0.0021 ± 0.0003
LbPFK[c]	0.020 ± 0.005	28 ± 8	nd[d]	24 ± 2	nd

[a] X and Y represent MgADP and PEP, respectively. [b] Data from ref 3. [c] Data fit to eq 4. [d] Not determined.

allosteric effect. Under such circumstances, the effects of an allosteric inhibitor can be assessed with a competitive inhibition model which reveals the dissociation constant of the inhibitor. The value of the K_{ix} obtained by fitting the data to eq 4 is presented in Table 1, as are the corresponding parameters for EcPFK and BsPFK. Decreasing the pH to 6 or 7 does not seem to change the amount of PEP inhibition (data not shown).

MgADP binding to the enzyme is also weak and, surprisingly, slightly inhibitory (Figure 3B). The extent of MgADP inhibition also cannot be determined due to experimental limitations and weak binding, so these data were also fit to eq 4 with the results also given in Table 1. PEP inhibition was examined in the presence of two concentrations of MgADP, and the binding affinity for PEP was observed to decrease as the concenetration of MgADP increases (data not shown), suggesting that MgADP binds to the allosteric site albeit very weakly. When the data for LbPFK are compared to those obtained for EcPFK and BsPFK (Table 1), it is notable that LbPFK and BsPFK both bind Fru-6-P with similar affinities, but the dissociation constants of LbPFK for PEP and MgADP are much larger than those for either EcPFK or BsPFK.

Structure Determination and Overall Structure. The crystals of phosphofructokinase from *L. bulgaricus* belong to space group $P6_222$ with unit cell dimensions of $a = 135.0$ Å and $c = 77.7$ Å, one subunit per asymmetric unit, and a solvent content of 58.7 %. The structure was determined by molecular replacement with *B. stearothermophilus* phosphofructokinase model (PDB ID: 6PFK, *17*). The final structure, including all the 319 residues, two sulfate molecules, and 252 water molecules, refined at 1.86 Å resolution, has a crystallographic *R*-value of 22.2% and an R_{free} of 25.1%. The details of the final refinement parameter are presented in Table 2.

The 319 residues in the LbPFK molecule form two structural domains, both with 3-layered αβα sandwich structures. The overall structure of the enzyme is very similar to that of EcPFK and BsPFK (*7*, *8*, *17*, *22*, *23*) as shown in Figure 4. Although there is only one molecule in the asymmetric unit, a 222 symmetry exists in the space group $P6_222$, suggesting that the oligomeric state of LbPFK is still tetramer and with 222 symmetry, very much like that of EcPFK (*8*, *22*) and BsPFK (*7*, *17*, *23*). The root-mean-square deviation (RMSD) between LbPFK and the so-called active R-state BsPFK (PDB ID: 3PFK and 4PFK, *7*, *23*) is 0.81 ± 0.01 Å for 319 Cα atoms, whereas that between LbPFK and the so-called inhibited T-state BsPFK (PDB ID: 6PFK, *18*) is 1.23 ± 0.03 Å for 319 Cα atoms. Further superimposition analysis on the tetramer shows that the RMSD between LbPFK tetramer and the active R-state BsPFK (PDB ID: 3PFK and 4PFK, *7*, *23*) tetramer is 0.90 Å for 1276 Cα atoms, whereas that between LbPFK tetramer and the inhibited T-state BsPFK (PDB ID: 6PFK, *17*) is 1.66 Å for 1276 Cα atoms, suggesting that the overall structure of LbPFK seems to correspond to the active R-state.

Table 2: Statistics from the Crystallographic Analysis[a]

data set	native
wavelength (Å)	1.0419
resolution (Å)	1.86
measured reflections	560 384
unique reflections	35567
redundancy	15.8
completeness (%, highest shell)	98.5 (92.8)
mean $I/\sigma I$ (highest shell)	50.6 (1.8)
R_{sym} (%, highest shell)	5.7 (69.8)
Refinement	
resolution (Å)	20.0−1.85
no. of reflections $\|F\| > 0\ \sigma F$	33708
R-factor/*R*-free (%)	22.4/25.6
no. of non-H atoms	2649
no. of sulfate molecules	2
no. of solvent atoms	259
rmsd bond lengths (Å)	0.009
rmsd bond angles (deg)	1.1
Ramachandran plot (%)	92.6
most favored regions	6.7
additional allowed regions	0.0
generously allowed regions	0.7
disallowed regions	

[a] For details of the crystallization and structure determination, see text. $R_{sym} = \sum_h\sum_i|I_{h,I} - I_h|/\sum_h\sum_i I_{h,I}$ for the intensity (I) of $\boldsymbol{i}$ observations of reflection h. *R*-factor $= \sum|F_{obs} - F_{calc}|/\sum|F_{obs}|$, where F_{obs} and F_{calc} are the observed and calculated structure factors, respectively. *R*-free = *R*-factor calculated by using a subset (~5%) of reflection data chosen ramdomly and omitted throughout refinement. rmsd, root-mean-square deviations from ideal geometry.

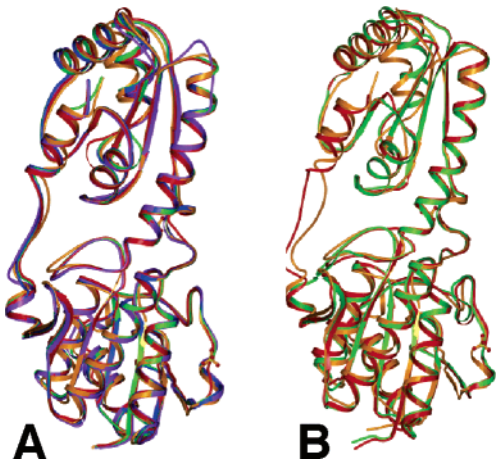

FIGURE 4: Comparison of the overall fold of LbPFK to the structures of EcPFK and BsPFK. (A) Superimposition of LbPFK (gold) with four BsPFK structures: 1MTO.pdb (red), 3PFK.pdb (green), 4PFK.pdb (blue), and 6PFK.pdb (purple). (B) Superimposition of LbPFK (gold) with two EcPFK structures: 1PFK.pdb (red) and 2PFK.pdb (green).

Binding Sites. The locations of three ligands have been identified in the structures of EcPFK and BsPFK: Fru-6-P and MgATP in the active site, and activator MgADP or

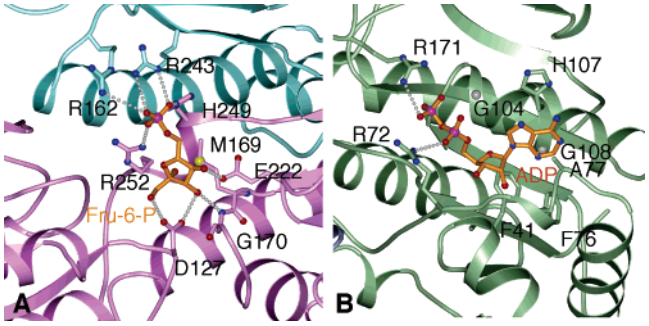

FIGURE 5: The active site of LbPFK. (A) The Fru-6-P binding site of LbPFK with Fru-6-P modeled in the site. (B) The ATP binding site of LbPFK with ADP modeled in the structure. Residues interacting with Fru-6-P and ADP are labeled.

allosteric inhibitor analogue phosphoglycolate in the allosteric site (*8*, *17*). In the LbPFK crystal structure, two inorganic sulfate ions from the crystallization condition were located, similar to the bound inorganic phosphate ions reported in BsPFK structure (*23*). One sulfate is bound in the active site, in correspondence with the 6-phosphate group of Fru-6-P, and the other one is bound in the allosteric site, in correspondence with the β-phosphate group of ADP or the phosphate group of phosphoglycolate.

The Active Site. Based on the bound sulfates in the LbPFK structure, and the available cocrystal structures of both BsPFK and EcPFK, a model was constructed with Fru-6-P and MgADP in the active site of LbPFK. The active site lies between the two domains of the subunit with the Fru-6-P binding site mainly formed in the small domain and the MgATP binding site in the large domain of LbPFK. All residues involved in Fru-6-P binding are strictly conserved in LbPFK (Figure 5A). These include Arg162, Arg243, His249, and Arg252 interacting with the 6-phosphate group of Fru-6-P, and Asp127, Met169, and Glu222 interacting with the sugar moiety of Fru-6-P. The bound inorganic sulfate forms salt bridges with His249 and Arg252 from one subunit, Arg162 and Arg243 from the other subunit, presumably stabilizing the LbPFK conformation to the active R-state. Residues involved in MgATP binding are also well conserved (Figure 5B). Two signature glycine residues (Gly104 and Gly108), which provide space for the ATP, and Arg72, which interacts with the α-phosphate of the ATP, are conserved. The side chains of Ala77, His107, Phe41, and Phe76, also conserved, still form a nonspecific hydrophobic slot for the adenine ring of ATP.

The Allosteric Site. The most obvious differences between the LbPFK, EcPFK, and BsPFK structures lie in the allosteric site (Figure 6). Studies with EcPFK (*8*) showed that the main interactions between PFK and activator MgADP are with the phosphate groups and the magnesium ion. The magnesium ion forms octahedral coordination with the α and β phosphate groups of ADP, the carbonyl oxygen of Gly185, the carboxyl of Glu187, and two water molecules (*8*). Glu187 is of special interest because the conformation of its side chain in BsPFK changes in the presence of activator or inhibitor in the allosteric site (*17*). In the active R-state, the side chain of Glu187 adopts a folded conformation, ready to be coordinated to the magnesium ion of ADP. In the inhibited T-state, the side chain χ_1 torsion angle of Glu187 changes by $\sim$140°, rotating away from the ligand. The new adopted position of the Glu187 side chain pushes the side chain of Leu205 to change its conformation. Glu187 also seems to influence the interaction of K213 with PEP. Glu187 has been proposed to be important for allosteric responsiveness in EcPFK (*24*−*26*). When substituted with an alanine at that position, PEP actually activates Fru-6-P binding in the presence of MgATP, whereas MgADP has no effect on Fru-6-P binding (*25*, *27*). In LbPFK, an aspartic residue is present at position 187. The octahedral coordination between the carboxyl of Asp187 and the magnesium might be very weak or no longer exists.

The residues involved in the interactions with the phosphate groups of ADP in EcPFK are Arg21, Arg25, Arg54, Arg154, and Lys213, whereas Arg21, Arg25, Arg154, Arg211, and Lys213 form similar interactions in BsPFK (*7*, *8*). Arg21, Arg25, Arg154, and Lys213 are conserved in LbPFK, whereas the corresponding residues for Arg54 and Arg211 are Ser54 and Ser211 in LbPFK. Furthermore, Asp59 in EcPFK and BsPFK forms a hydrogen bond with the ribose O_3. A histidine residue is present at position 59 in LbPFK, which might break the interaction, further decreasing the affinity between LbPFK and ADP in allosteric site. Moreover, the stacking interactions that exist between Tyr55 and ADP in EcPFK could be disrupted in LbPFK in which a glutamate exists at that position. Finally, the effect of the change from Lys214 in EcPFK and BsPFK to Asp in LbPFK is not clear.

DISCUSSION

Our kinetic characterization of phosphofructokinase from *L. bulgaricus* indicates properties that differ from those obtained by Le Bras et al. (*9*). These discrepancies may be due to the presence of the monovalent cation NH_4^+ and the fact that we performed our assays at higher a MgATP concentration to ensure full saturation. We introduced these modifications to our assays in order to be consistent with

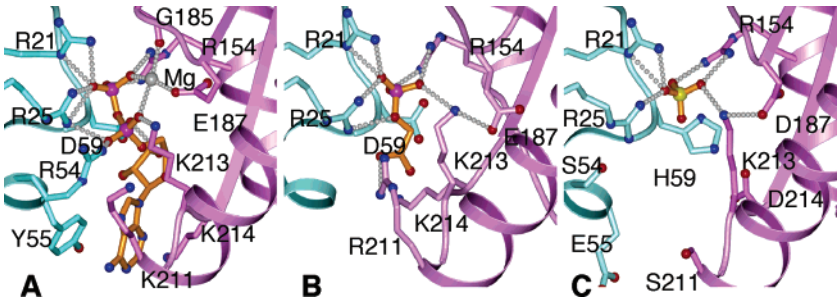

FIGURE 6: Comparison of the allosteric sites of PFK with different ligands present. (A) MgADP-bound EcPFK. (B) Phosphoglycolate-bound BsPFK. (C) Sulfate-bound LbPFK.

the assays of EcPFK reported in the literature. The data we obtained reveals an enzyme that binds substrates MgATP and Fru-6-P with dissociation constants of 0.35 ± 0.01 mM and 0.020 ± 0.001 mM, respectively, and with a maximal specific activity of 240 ± 10 units/mg at pH 8.0 at 25 °C. The apparent affinity for Fru-6-P diminishes somewhat at lower pH values; however, the small effects of PEP and MgADP are evident at pH 6 as well as pH 8.

Although LbPFK is less perturbed by PEP and MgADP than either EcPFK or BsPFK, it is not correct to conclude that LbPFK has no allosteric properties. Rather a small amount of inhibition by both PEP and MgADP is evident at high concentrations of each ligand, although the effect of MgADP is barely detectible. Because of the apparent weakness of the binding of these ligands ($K_d \sim 20$ mM), the extent of inhibition cannot be determined, although the data are consistent with both ligands binding to the same site as is the case for both EcPFK and BsPFK. The structure of LbPFK provides a rationale for these weak interactions.

The crystal structure of LbPFK was solved to 1.86 Å resolution. The overall fold is conserved between EcPFK, BsPFK, and LbPFK. The active site of LbPFK remains intact, whereas most differences lie within the allosteric sites of the structures of EcPFK, BsPFK, and LbPFK. The tight binding of Fru-6-P to LbPFK is similar to that of BsPFK, which is not surprising since the active sites of both enzymes are similar. The weak binding of MgADP and PEP observed for LbPFK compared to their affinities for EcPFK likely involves the differences in the residues lining the allosteric site. However, the structure of LdPFK itself does not provide a clear answer to why the effects of MgADP and PEP on Fru-6-P binding are both inhibitory in LbPFK. It is possible that, given the differences in the binding site relative to EcPFK, MgADP might bind in an orientation that produces effects more comparable to PEP than occurs with the *E. coli* enzyme.

Although a small degree of inhibition is observed with PEP, an observation that suggests that PEP inhibition may not play a role in the physiological regulation of this enzyme, the weak binding of PEP prevents the assessment of whether poor binding is the primary defect or whether the enzyme would be poorly responsive were PEP able to bind. The previous conclusion that LbPFK is "nonallosteric" conveys the impression that the latter circumstance is the case. However, only the coupling constant quantitatively conveys the actual degree of allosteric responsiveness biophysically. In the absence of PEP saturation, the magnitude of the coupling between PEP and Fru-6-P cannot be measured. We have previously observed numerous mutants of EcPFK, generated by site-directed mutagenesis, that greatly diminish binding of Fru-6-P without diminishing appreciably the coupling between Fru-6-P and either allosteric ligand (*28*). It is possible that such is the case here. In this regard it may be significant that so little of the structure of LbPFK appears to be different from that of BsPFK (and EcPFK) except in the vicinity of the binding site for PEP. MgADP binding to this same site is also weaker, and slightly inhibitory, suggesting that the structural elements necessary for conveying activation are also missing. However, we cannot rule out that MgADP merely binds weakly in an "incorrect" orientation, thereby failing to produce the usual effect.

REFERENCES

1. Blangy, D. H., Buc, H., and Monod, J. (1968) Kinetics of the allosteric interactions of phosphofructokinase from *Escherichia coli*, *J. Mol. Biol. 31*, 13−35.
2. Uyeda, K. (1979) Phosphofructokinase, *Adv. Enzymol. 48*, 193−224.
3. Tlapak-Simmons, V. L., and Reinhart, G. D. (1998) Obfuscation of allosteric structure-function relationships by enthalpy-entropy compensation, *Biophys. J. 75*, 1010−1015.
4. Johnson, J. L., and Reinhart, G. D. (1994) Influence of MgADP on phosphofructokinase from *Escherichia coli*. Elucidation of coupling interactions with both substrates, *Biochemistry 3*, 2635−2643.
5. Johnson, J. L., and Reinhart, G. D. (1997) Failure of a two-state model to describe the influence of phospho(enol)pyruvate on phosphofructokinase from *Escherichia coli*, *Biochemistry 36*, 12814−12822.
6. Deville-Bonne, D., Laine, R., and Garel, J. R. (1991) Substrate antagonism in the kinetic mechanism of *E. coli* phosphofructokinase-1, *FEBS Lett. 290*, 173−176.
7. Evans, P. R., Farrants, G. W., and Hudson, P. J. (1981) Phosphofructokinase: structure and control, *Philos. Trans. R. Soc. London B 293*, 53−62.
8. Shirakihara, Y., and Evans, P. R. (1988) Crystal structure of the complex of phosphofructokinase from *Escherichia coli* with its reaction products, *J. Mol. Biol. 204*, 973−994.
9. Le Bras, G., Deville-Bonne, D., and Garel, J. R. (1991) Purification and properties of the phosphofructokinase from *Lactobacillus bulgaricus*. A non-allosteric analog of the enzyme from *Escherichia coli*, *Eur. J. Biochem. 198*, 683−687.
10. Reinhart, G. D. (1983) The determination of thermodynamic allosteric parameters of an enzyme undergoing steady-state turnover, *Arch. Biochem. Biophys. 224*, 389−401.
11. Reinhart, G. D. (1988) Linked-function origins or cooperativity in a symmetrical dimer, *Biophys. Chem. 30*, 159−172.
12. Branny, P., De La Torre, F., and Garel, J. R. (1993) Cloning, sequencing, and expression in *Escherichia* coli of the gene coding for phosphofructokinase from *Lactobacillus bulgaricus*, *J. Bacteriol. 175*, 5344−5379.
13. Daldal, F. (1983) Molecular cloning of the gene for phosphofructokinase-2 of *Escherichia coli* and the nature of a mutation, pfkB1, causing a high level of the enzyme, *J. Mol. Biol. 168*, 285−305.
14. Cleland, W. W. (1986) Enzyme kinetics as a tool for determination of enzyme mechanisms, in *Investigations of Rates and Mechanisms of Reactions* (Bernasconi, C. F., Ed.) pp 791−870, John Wiley & Sons, New York.
15. Otwinowski, Z., and Minor, W. (1997) Processing of x-ray diffraction data collected in oscillation mode, *Methods Enzymol. 276*, 307−326.
16. Collaborative Computational Project, N. (1994) The CCP4 suite: programs for protein crystallography, *Acta Crystallogr., Sect. D: Biol. Crystallogr. 50*, 760−763.
17. Schirmer, T., and Evans, P. R. (1990) Structural basis of the allosteric behavior of phosphofructokinase, *Nature 343*, 140−145.
18. McRee, D. E. (1999) XtalView/Xfit: A versatile program for manipulating atomic coordinated and electron density, *J. Struct. Biol. 125*, 156−165.
19. Perrakis, A., Harkiolaki, M., Wilson, K. S., and Lamzin, V. S. (2001) ARP/warp and molecular replacement, *Acta Crystallogr., Sect. D: Biol. Crystallogr. 57*, 1445−1450.
20. Johnson, J. L., and Reinhart, G. D. (1992) MgATP and Fructose 6-Phosphate Interactions with Phosphofructokinase from *E. coli*, *Biochemistry 31*, 11510−11518.
21. Byrnes, M. X., Zhu, X., Younathan, E. S., and Chang, S. H. (1994) *Biochemistry 33*, 3424−3431.
22. Rypniewski, W. R., and Evans, P. R. (1989) Crystal structure of unliganded phosphofructokinase from *Escherichia coli*. *J. Mol. Biol. 207*, 805−821.
23. Evans, P. R., and Hudson, P. J. (1979) Structure and control of phosphofructokinase from *Bacillus stearothermophilus*, *Nature 279*, 500−504.

24. Auzat, I., Le Bras, G., Branny, P., De La Torre, F., Theunissen, B., and Garel, J. R. (1994) The role of Glu187 in the regulation of phosphofructokinase by phosphoenolpyruvate, *J. Mol. Biol. 235*, 68−72.
25. Lau, F. T., and Fersht, A. R. (1987) Conversion of allosteric inhibition to activation in phosphofructokinase by protein engineering, *Nature 326*, 811−812.
26. Lau, F. T., and Fersht, A. R. (1989) Dissection of the effector-binding site and complementation studies of *Escherichia coli* phosphofructokinase using site-directed mutagenesis, *Biochemistry 28*, 6841−6847.
27. Pham, A. S., Tlapak-Simmons, F., and Reinhart, G. D. (2001) Persistent binding of MgADP to the E187A mutant of *Escherichia coli* phosphofructokinase in the absence of allosteric effects, *Biochemistry 40*, 4140−4149.
28. Fenton, A. W., Paricharttanakul, N. M., and Reinhart, G. D. (2003) Identification of Substrate Contact Residues Important for the Allosteric Regulation of Phosphofructokinase for *Escherichia coli*, *Biochemistry 42*, 6453−6459.

BI051283G